

Online Supplement

Endothelin-1 critically contribute to EPC reduction and dysfunction via an ET_A/NADPH oxidase pathway-induced oxidative stress in salt-sensitive hypertension

Dan-Dan Chen,^{1,2} Yu-Gang Dong,² Alex F. Chen.¹

¹Department of Surgery, University of Pittsburgh School of Medicine, Pittsburgh, PA 15213, and Vascular Surgery Research, Veterans Affairs Pittsburgh Healthcare System, Pittsburgh, PA 15240, USA; ²Department of Cardiology, The First Affiliated Hospital of Sun Yat-Sen University, Guangzhou, 510080, P.R. China

Running title: ET-1, EPC reduction and dysfunction in hypertension

Correspondance:

Alex F. Chen, MD, PhD
Department of Surgery
University of Pittsburgh School of Medicine
W1148 Biomedical Science Tower
200 Lothrop Street
Pittsburgh, PA, 15213

Tel: 412-624-6869

Fax: 412-648-7107

E-mail: chena5@upmc.edu

Authorship Note: Dan-Dan Chen and Yu-Gang Dong share first authorship.

Supplemental Methods

All the procedures in this study were approved by the University of Pittsburgh Institutional Animal Care and Use Committee and were performed in accordance with the National Institutes of Health Guide for the Care and Use of Laboratory Animals.

Animals

All male Sprague-Dawley (SD) rats (250-285 g) were obtained from Charles River Laboratories. Breeding pairs of ET_B receptor deficiency (*DBH;ET_B^{sl/sl}, ET_B^{-/-}*) rats and ET_B wild-type (*DBH;ET_B^{+/+}, ET_B^{+/+}*) rats were a generous gift from Dr. Cheryl E. Garipey (University of Michigan, Ann Arbor, MI)⁵. In the present study, male ET_B^{-/-} and ET_B^{+/+} rats (240-280 g) were used. ET_B^{-/-} rats are a novel single-locus genetic model of severe salt-sensitive hypertension, which express ET_B receptors in adrenal glands and other adrenergic neurons but not in other tissues, such as the kidney, vascular endothelium, and vascular smooth muscle⁵.

DOCA-salt hypertensive rats and in vivo pharmacologic intervention

DOCA-salt hypertension was created in adult male SD rats as we previously described⁶⁻⁸. From the beginning of DOCA administration, some DOCA-salt rats received 4 weeks of ABT-627 (5 mg·kg⁻¹·d⁻¹ in drinking water, Abbott Laboratories), a selective ET_A receptor antagonist⁹. Some DOCA-salt rats received diuretic trichlormethiazide (TCM, 10 mg·kg⁻¹·d⁻¹ in drinking water, Sigma)¹⁰. Some DOCA-salt rats received Apocynin (1.5 mmol/L in drinking water, Sigma), a NADPH oxidase inhibitor that impedes the assembly of the p47^{phox} and p67^{phox} within the membrane NADPH oxidase complex^{7, 11, 12}. Our previous studies have shown that these doses of ABT-627 and Apocynin are effective in blocking the ET_A receptors and the NADPH oxidase activity in vivo, respectively^{8, 9, 11}. Average systolic blood pressure (SBP) of Sham and DOCA-salt rats was measured by the non-invasive tail-cuff method in conscious rats⁶⁻⁸. The peripheral blood of some rats was collected when the blood pressure was significantly elevated on Day 5 after DOCA-salt regimen. The peripheral blood and bone marrow of other rats were collected at Day 28 (4 weeks) following DOCA-salt regimen. The blood pressure of ET_B^{-/-} rats was monitored by radiotelemetry as we described previously¹³. Briefly, arterial blood pressure was monitored remotely using a commercially available radiotelemetry data acquisition program (Dataquest ART 3.1, Data Sciences International). Data were reported as 24-hour averages.

EPC isolation and characterization

Bone marrow-derived EPCs (BM-EPCs) were isolated from the femur and tibia of rats according to our recent publications¹⁻⁴. All assays were performed after day 7. BM-EPCs were used in EPC function assays, Western blot analysis, NADPH oxidase activity and cell implantation. Freshly isolated MNCs and cultured BM-EPCs were characterized by flow cytometry according to our recent publications^{1, 3, 4, 14}. To detect CD133, Flk-1, and VE-Cadherin, cells were incubated with rabbit anti-rat CD133 antibodies (Abcam), or rabbit anti-rat Flk-1 antibodies (Abcam), or mouse anti-rat VE-Cadherin antibodies (Santa Cruz) on ice for one hour right after pre-permeabilization with fresh-prepared methanol for 15 minutes. Then, cells were incubated with FITC-conjugated goat anti-rabbit secondary antibodies (Abcam) or PE-conjugated goat anti-mouse secondary antibodies (Santa Cruz) on ice for another one hour. 0.5% rabbit serum or 0.5% mouse serum was used for isotype staining. To detect CD34 or CD45, cells were incubated with mouse anti-rat CD34-PE antibodies (Santa Cruz) or mouse anti-rat CD45-PECy5 antibodies (BD Bioscience) on ice for one hour. Isotype specific conjugated anti-IgG was used as negative control. Quantifications of CD34+/Flk-1+ cells, CD34+/CD133+ cells, CD34+ cells, CD133+ cells, Flk-1+ cells, VE-Cadherin+ cells, and

CD45+ cells were performed with a BD Vantage Flow Cytometer. Each analysis included at least 10,000 events.

Expressions of ET_A and ET_B receptors in EPCs by real-time PCR, immunocytochemistry, and Western blot analysis

ET_A and ET_B receptors on EPC were assessed by real-time RT-PCR, immunocytochemistry, and Western blot as described previously¹⁵. For all experiments, 18s was used as an internal control. The specific primer sequences were as follows: ET_A receptor, forward: CCTGGCAACCATGAACTCTTGCAT; reverse: TGGACTGGTGACAACAGCAACAGA; ET_B receptor, forward: ATTCTGAAGCTCACCTTTATGAC; reverse: AGAAGCCATGTTGATATCCAATGTA; and 18s, forward: GGGCCCGAAGCGTTTACTTTGAA; reverse: ACCGCGGTCCTATTCCATTATTC. Amplification was performed on a 7500 Real-Time PCR system (Applied Biosystems) according to the manufacturer's instructions. Relative mRNA expressions of the ET_A and ET_B receptors were calculated by the comparative C_T method, normalized to the endogenous 18s control, and calculated as a relative expression= $2^{-\Delta\text{ct}}$ ¹. For immunocytochemistry, cells were fixed with 4% PFA in PBS for 20 minutes at room temperature¹⁵. Antibodies against the ET_A and ET_B receptors were from Alomone (Jerusalem, Israel). To verify the specificity of antibody binding, the primary antibody was incubated with the control peptide prior to application to cells. The absence of immunoreactivity confirmed the specificity of antibodies for ET receptors. The images were taken with a Zeiss Pascal confocal microscope at a resolution of 1,024×1,024 pixels.

Western blots were performed by using primary antibodies directed against ET_A receptors (1:200 dilution; Alomone Labs) and ET_B receptors (1:200 dilution; Alomone Labs). To verify equal protein loading and transfer, the β -actin (1:10,000 dilution; Sigma) was used as the internal control. Bands were visualized with an Odyssey Imager and quantified with Quantity One software (Bio-Rad)¹⁵.

EPC angiogenic function assays and pharmacologic treatments

EPC angiogenic function assays including tube formation capacity by Matrigel assay and adhesion function assay were described in detail in our previous studies^{1,3,4}.

In vitro gene transfer

The propagation, purification, and titration of replication-incompetent adenoviral vectors were prepared as we described^{7,16}. After 7-days in culture, EPCs were transfected with the adenoviral vector encoding dominant-negative Rac1 (DNRac1) that inhibits endogenous NADPH oxidase subunit Rac1¹⁶ or reporter gene β -galactosidase (β -gal) at a titer of 500 multiplicity of infection (MOI) in EGM-2 supplemented with 2% fetal bovine serum for 24 hours, followed by change of fresh 5% FBS EGM-2¹. After 48 more hours of cultivation, transfected EPCs were subjected to ET-1 treatment as described above¹⁶.

Circulating EPC flow cytometry

Circulating EPCs were isolated according to our published methods^{1,3}. Briefly, freshly isolated peripheral blood mononuclear cells (PB-MNCs, 1×10^6 cells) were incubated with Flk-1 (2 $\mu\text{g}/10^6$ cells, Abcam) for one hour on ice, then incubated with a biotin-labeled goat anti-mouse IgG antibody (2.6 $\mu\text{g}/10^6$ cells, Jackson Immuno Research) for 30 minutes, followed by one hour incubation with APC-conjugated streptavidin (20 $\mu\text{l}/10^6$ cells, BD Biosciences) and PE-conjugated CD34 (1 $\mu\text{g}/10^6$ cells, Santa Cruz) on ice¹⁷. After washing and centrifugation, the cell pellets were suspended in 500 μl 5% BSA-PBS, and co-expressions of CD34 and Flk-1 were determined by flow cytometry

(FACScan, Becton Dickinson) gating 30,000 events. Isotype specific conjugated anti-IgG was used as negative control.

Intracellular ROS measurement with dichlorofluorescein fluorescence (DCF) by flow cytometry

The intracellular ROS level in circulating EPCs was evaluated by DCF fluorescence using flow cytometry according to the manufacturer's recommended protocol and previous publications^{18, 19}. 5-(6)-chloromethyl-2',7'-dichlorodihydrofluorescein diacetate (CM-H₂DCFDA) enters the cells and produces a green fluorescent signal (DCF fluorescence) after intracellular oxidation by ROS. The DCF/CD34/Flk-1 triple-positive cells were determined by flow cytometry (FACScan, Becton Dickinson) gating 30,000 events. The mean fluorescence of DCF was taken as an indicator of intracellular ROS level in circulating CD34⁺/Flk-1⁺ progenitor cells.

NADPH oxidase enzymatic activity

NADPH oxidase activity in EPCs was measured by a lucigenin-enhanced chemiluminescence assay, as we described with minor modifications^{6, 20, 21}. Briefly, the enzyme activity was measured by lucigenin (5×10^{-6} mol/L, Sigma) and indicated as the amount of O₂⁻ levels in the presence of their relative substrate NADPH (1×10^{-4} mol/L, Sigma)⁶. No enzymatic activity could be detected in the absence of NADPH.

Western blot analyses

Western blots were performed by using primary antibodies directed against Rac1 (1:1,000 dilution; Abcam), gp91^{phox} (1:1,000 dilution; BD Biosciences), p22^{phox} (1:500 dilution; Santa Cruz), MnSOD (1:1,000 dilution; BD Biosciences), CuZnSOD (1:10,000 dilution; Abcam), catalase (1:1,000 dilution; BD Biosciences), GPx-1 (1:500 dilution; Santa Cruz), p53 (1:2,500 dilution; Cell Signals), Bcl-2 (1:1,000 dilution; BD Biosciences), and Bax (1:1,000 dilution; BD Biosciences). To verify equal protein loading and transfer, β -actin (1:10,000 dilution; Sigma) was used as the internal control. Bands were visualized with an Odyssey Imager and quantified with Quantity One software (Bio-Rad)^{1, 3, 4, 14}.

Senescence assay

EPC senescence was determined by acidic β -galactosidase staining kit (Sigma), according to the manufacturer's recommended protocol and our recent publication⁴.

Apoptosis assay

EPC apoptosis was determined by DeadEnd Fluorometric TUNEL System staining (Promega) according to the manufacturer's instructions²². Cell nuclei were co-stained with the fluorescent dye Hoechst33528¹. The green-staining nuclei (TUNEL-positive cells) were detected under a fluorescence microscope equipped with a digital camera and the MetaMorph 6.1 image analysis software (Universal Imaging Corporation)²². TUNEL-positive cells were counted under ten random high power fields (magnifications 200 \times) of each sample.

Telomerase activity

Telomeric Repeat Amplification Protocol Assay (TRAP Assay) was employed, through which the telomerase reaction product is amplified by PCR²³. Telomerase activity was measured with 2 μ g proteins by the Telo TAGGG Telomerase PCR ELISA^{plus} Kit (Roche, USA) according to the manufacturer's instructions²³. The absorbance values were determined by using a Micro-plate reader; the absorbance of the samples was measured at 450 nm wavelengths.

Hindlimb ischemia and in vivo EPC therapy

Hindlimb ischemia was carried out in Sham or DOCA-salt rats on Day 14 after DOCA or Sham surgery. Briefly, the right femoral artery and its branches were exposed proximal to the origin of the arterial popliteal, ligated, and the incision was closed in layers. The left femoral artery and its branches were only exposed without dissection, which served as non-ischemia control^{24, 25}. DOCA-salt rats were randomly divided into five groups, which received PBS (vehicle) or BrdU-labeled EPC implantation: 1) DOCA rats + PBS, 2) DOCA rats + sham rat-derived EPCs (Sham-EPCs), 3) DOCA rats + DOCA rat-derived EPCs (DOCA-EPCs), 4) DOCA rats + ABT treated DOCA rat-derived EPCs (ABT-EPCs), and 5) DOCA rats + DNRac-1 treated DOCA rat-derived EPCs (DNRac1-EPCs). In the vehicle or EPC implantation groups, 100 μ l of PBS or 1×10^7 EPCs in 100 μ l, was randomly injected intramuscularly into anterior tibial muscle at the six points with a 27-gauge needle 24 hours after femoral artery dissection²⁵. Hindlimb blood flow was measured before, right after, 7 days after, and 14 days after right femoral artery ligations. The rats were pre-warmed for 10 minutes, and then placed on 37°C heated pads through the measurement²⁶. The hindlimb blood flow was measured by a Laser Doppler Perfusion Imager (LDPI) as described previously²⁴. Low or no perfusion is displayed as dark blue, whereas the high perfusion is displayed as yellow or red. The blood flow images were measured with Image-Pro Plug 5.0 and expressed as perfusion ratio of ischemic hindlimb to non-ischemic limb.

Immunohistochemistry and measurement of capillary density

The effect of EPC implantation (or PBS) on neovascularization was assessed under light microscopy by measuring of the number of capillaries in sections taken from the ischemic muscles^{24, 25}. Tissue specimens were obtained from anterior tibial muscles on day 14. This muscle was chosen because it is one of the principal muscles of the lower limb and is commonly used to evaluate the distal reperfusion after the femoral arteries are excised. The muscle was fixed in 10% Formalin and embedded in paraffin. Sections (5 μ m) were de-paraffinized and incubated with a goat anti-human CD31 antibody (1:100 dilution, Santa Cruz). Antibody distribution was visualized with the use of the avidin-biotin-complex technique and Vector Red chromogenic substrate (Vector Laboratories), followed by counterstaining with hematoxylin. Negative controls were performed by avoiding the primary antibodies. Capillaries were identified by positive staining for CD31. Five fields from each sample were randomly selected and photographed with a digital camera (Olympus), and visible capillaries (positive for CD31) were counted. Capillary density was expressed as the number of capillaries per square millimeter²⁷. To investigate whether implanted EPCs were incorporated the capillaries, BrdU labeled EPCs were injected intramuscularly into anterior tibial muscle. On Day 14, the anterior tibial muscle was collected and fixed with 10% Formalin. The sections were incubated with BrdU antibody (1:50 dilution, Amersham Biosciences) and CD31 antibody (1:50 dilution, Santa Cruz), followed by secondary antibodies anti-mouse PE and anti-goat FITC, respectively. Implanted EPCs were identified as BrdU positive cells²⁸.

Data analysis

All obtained values were expressed as mean \pm SEM. A GraphPad Prism (Version 5) was used for data analysis. Statistical analysis between two groups was performed using the Student's two-tailed unpaired t test. A one-way ANOVA was used in data analysis when more than two groups were compared, followed by the Bonferroni's procedure to control the Type I error. A two-way Repeated-measures ANOVA followed by the Bonferroni's post-test was used to analyze blood flow perfusion in hindlimb ischemia models, and a significant overall difference was detected 10, 16. Specifically, the group of DOCA-salt rats was compared with the Sham group, to determine the effect

of DOCA-salt treatment on EPC functions and subsequent molecular changes. The groups of ABT-627 + DOCA and Apocynin + DOCA were compared with DOCA-salt rats to determine the effects of the blockade of ET_A/NADPH oxidase pathway on EPC functions and subsequent molecular changes. A value of P<0.05 was considered as a statistically significant finding.

References

1. Marrotte E, Chen DD, Hakim JS, Chen AF. Restoration of endothelial progenitor cell function with manganese superoxide dismutase accelerates wound healing in diabetic mice. *J Clin Invest*. 2010;120:4207-4219.
2. Wang XR, Zhang MW, Chen DD, Zhang Y, Chen AF. AMPK rescues the angiogenic functions of endothelial progenitor cells via manganese superoxide dismutase induction in type 1 diabetes. *Am J Physiol Endocrinol Metab*. 2011;300:E1135-1145.
3. Xie HH, Zhou S, Chen DD, Channon KM, Su DF, Chen AF. GTP Cyclohydrolase I/BH4 Pathway Protects EPCs via Suppressing Oxidative Stress and Thrombospondin-1 in Salt-sensitive Hypertension. *Hypertension*. 2010;56:1137-1144.
4. Zhao T, Li J, Chen AF. MicroRNA-34a induces endothelial progenitor cell senescence and impedes its angiogenesis via suppressing silent information regulator 1. *Am J Physiol Endocrinol Metab*. 2010;299:E110-116.
5. Gariepy CE, Ohuchi T, Williams SC, Richardson JA, Yanagisawa M. Salt-sensitive hypertension in endothelin-B receptor-deficient rats. *J Clin Invest*. 2000;105:925-933.
6. Li L, Chu Y, Fink GD, Engelhardt JF, Heistad DD, Chen AF. Endothelin-1 stimulates arterial VCAM-1 expression via NADPH oxidase-derived superoxide in mineralocorticoid hypertension. *Hypertension*. 2003;42:997-1003.
7. Li L, Fink GD, Watts SW, Northcott CA, Galligan JJ, Pagano PJ, Chen AF. Endothelin-1 increases vascular superoxide via endothelin(A)-NADPH oxidase pathway in low-renin hypertension. *Circulation*. 2003;107:1053-1058.
8. Li L, Watts SW, Banes AK, Galligan JJ, Fink GD, Chen AF. NADPH oxidase-derived superoxide augments endothelin-1-induced vasoconstriction in mineralocorticoid hypertension. *Hypertension*. 2003;42:316-321.
9. Wang Y, Chen AF, Wang DH. ET(A) receptor blockade prevents renal dysfunction in salt-sensitive hypertension induced by sensory denervation. *Am J Physiol Heart Circ Physiol*. 2005;289:H2005-2011.
10. Yu Y, Fukuda N, Yao EH, Matsumoto T, Kobayashi N, Suzuki R, Tahira Y, Ueno T, Matsumoto K. Effects of an ARB on endothelial progenitor cell function and cardiovascular oxidation in hypertension. *Am J Hypertens*. 2008;21:72-77.
11. Beswick RA, Dorrance AM, Leite R, Webb RC. NADH/NADPH oxidase and enhanced superoxide production in the mineralocorticoid hypertensive rat. *Hypertension*. 2001;38:1107-1111.
12. Meyer J. Miraculous catch of iron-sulfur protein sequences in the Sargasso Sea. *FEBS Lett*. 2004;570:1-6.
13. King AJ, Osborn JW, Fink GD. Splanchnic circulation is a critical neural target in angiotensin II salt hypertension in rats. *Hypertension*. 2007;50:547-556.
14. Wang X, Chen J, Tao Q, Zhu J, Shang Y. Effects of ox-LDL on number and activity of circulating endothelial progenitor cells. *Drug Chem Toxicol*. 2004;27:243-255.
15. Dai X, Galligan JJ. Differential trafficking and desensitization of human ET(A) and ET(B) receptors expressed in HEK 293 cells. *Exp Biol Med (Maywood)*. 2006;231:746-751.
16. Li L, Crockett E, Wang DH, Galligan JJ, Fink GD, Chen AF. Gene transfer of endothelial NO synthase and manganese superoxide dismutase on arterial vascular cell adhesion molecule-1

expression and superoxide production in deoxycorticosterone acetate-salt hypertension. *Arterioscler Thromb Vasc Biol.* 2002;22:249-255.

17. Thum T, Fraccarollo D, Galuppo P, Tsikas D, Frantz S, Ertl G, Bauersachs J. Bone marrow molecular alterations after myocardial infarction: Impact on endothelial progenitor cells. *Cardiovasc Res.* 2006;70:50-60.
18. Miyazawa N, Abe M, Souma T, Tanemoto M, Abe T, Nakayama M, Ito S. Methylglyoxal augments intracellular oxidative stress in human aortic endothelial cells. *Free Radic Res.* 2010;44:101-107.
19. Obrosova IG, Pacher P, Szabo C, Zsengeller Z, Hirooka H, Stevens MJ, Yorek MA. Aldose reductase inhibition counteracts oxidative-nitrosative stress and poly(ADP-ribose) polymerase activation in tissue sites for diabetes complications. *Diabetes.* 2005;54:234-242.
20. Werner C, Kamani CH, Gensch C, Bohm M, Laufs U. The peroxisome proliferator-activated receptor-gamma agonist pioglitazone increases number and function of endothelial progenitor cells in patients with coronary artery disease and normal glucose tolerance. *Diabetes.* 2007;56:2609-2615.
21. Minkenberg I, Ferber E. Lucigenin-dependent chemiluminescence as a new assay for NAD(P)H-oxidase activity in particulate fractions of human polymorphonuclear leukocytes. *Journal of immunological methods.* 1984;71:61-67.
22. Verma S, Kuliszewski MA, Li SH, Szmítko PE, Zucco L, Wang CH, Badiwala MV, Mickle DA, Weisel RD, Fedak PW, Stewart DJ, Kutryk MJ. C-reactive protein attenuates endothelial progenitor cell survival, differentiation, and function: further evidence of a mechanistic link between C-reactive protein and cardiovascular disease. *Circulation.* 2004;109:2058-2067.
23. Assmus B, Urbich C, Aicher A, Hofmann WK, Haendeler J, Rossig L, Spyridopoulos I, Zeiher AM, Dimmeler S. HMG-CoA reductase inhibitors reduce senescence and increase proliferation of endothelial progenitor cells via regulation of cell cycle regulatory genes. *Circ Res.* 2003;92:1049-1055.
24. You D, Cochain C, Loinard C, Vilar J, Mees B, Duriez M, Levy BI, Silvestre JS. Hypertension impairs postnatal vasculogenesis: role of antihypertensive agents. *Hypertension.* 2008;51:1537-1544.
25. Ikenaga S, Hamano K, Nishida M, Kobayashi T, Li TS, Kobayashi S, Matsuzaki M, Zempo N, Esato K. Autologous bone marrow implantation induced angiogenesis and improved deteriorated exercise capacity in a rat ischemic hindlimb model. *J Surg Res.* 2001;96:277-283.
26. Kuhn M, Volker K, Schwarz K, Carbajo-Lozoya J, Fogel U, Jacoby C, Stypmann J, van Eickels M, Gambaryan S, Hartmann M, Werner M, Wieland T, Schrader J, Baba HA. The natriuretic peptide/guanylyl cyclase--a system functions as a stress-responsive regulator of angiogenesis in mice. *J Clin Invest.* 2009;119:2019-2030.
27. Huang PH, Chen YH, Wang CH, Chen JS, Tsai HY, Lin FY, Lo WY, Wu TC, Sata M, Chen JW, Lin SJ. Matrix metalloproteinase-9 is essential for ischemia-induced neovascularization by modulating bone marrow-derived endothelial progenitor cells. *Arterioscler Thromb Vasc Biol.* 2009;29:1179-1184.
28. Jiang J, Wang J, Li C, Yu SP, Wei L. Dual roles of tumor necrosis factor-alpha receptor-1 in a mouse model of hindlimb ischemia. *Vasc Med.* 2009;14:37-46.

Results

Characterization of bone marrow-derived EPCs

To characterize bone marrow derived EPCs, the stem cell markers (CD34, CD133), endothelial cell markers (Flk-1, VE-cadherin) and a hematopoietic cell marker (CD45) were examined by flow cytometry according to the procedure described in our recent publications¹⁻⁴. The cell populations were showed in Supplemental Table 1 and Table 2. These data suggest that EPCs cultured for 7 days (termed as early-cultured EPCs) are heterogeneous in nature, and they contain significantly higher percentage of progenitor cells with endothelial differentiating potential compared with the freshly isolated mononuclear cells. The early-cultured EPCs were also identified by Dil-acLDL/lectin double staining (Supplemental Fig. S3A) and the expressions of endothelial lineage markers between HUVECs and EPCs cultured for 7 days. Similar to HUVECs, early-cultured EPCs expressed endothelial markers including Flk-1, VE-cadherin, and eNOS (Supplemental Fig. S3B).

Supplemental Tables

Table S1. The cell population of freshly isolated mononuclear cells.

Cell surface markers	Sham (n=7)	DOCA (n=7)
CD34	17.65±4.98	13.84±2.40
CD133	39.51±7.38	25.71±5.30
Flk-1	8.98±2.23	5.51±1.72
VE-cadherin	2.84±0.87	2.92±1.60
CD34/CD133	3.36±0.46	2.60±0.35
CD34/Flk-1	3.64±0.64	4.03±1.79
CD45	53.37±3.91	41.97±5.89

MNCs (Day 0): freshly isolated mononuclear cells; EPCs (Day 7): 7-day cultured endothelial progenitor cells. The data were expressed as mean ± SEM, n=7 each group.

Table S2. The cell population of 7-day cultured EPCs.

Cell surface markers	Sham (n=7)	DOCA (n=7)
CD34	31.91±2.50	24.90±3.04
CD133	20.50±1.20	14.99±3.52
Flk-1	19.32±2.91	17.8±3.96
VE-cadherin	10.72±0.35	7.74±1.54
CD34/CD133	20.02±1.12	13.13±6.80
CD34/Flk-1	15.9±1.39	12.76±2.43
CD45	9.98±3.45	13.60±4.15

The data were expressed as mean ± SEM, n=7 each group.

Supplemental Figures

Fig. S1.

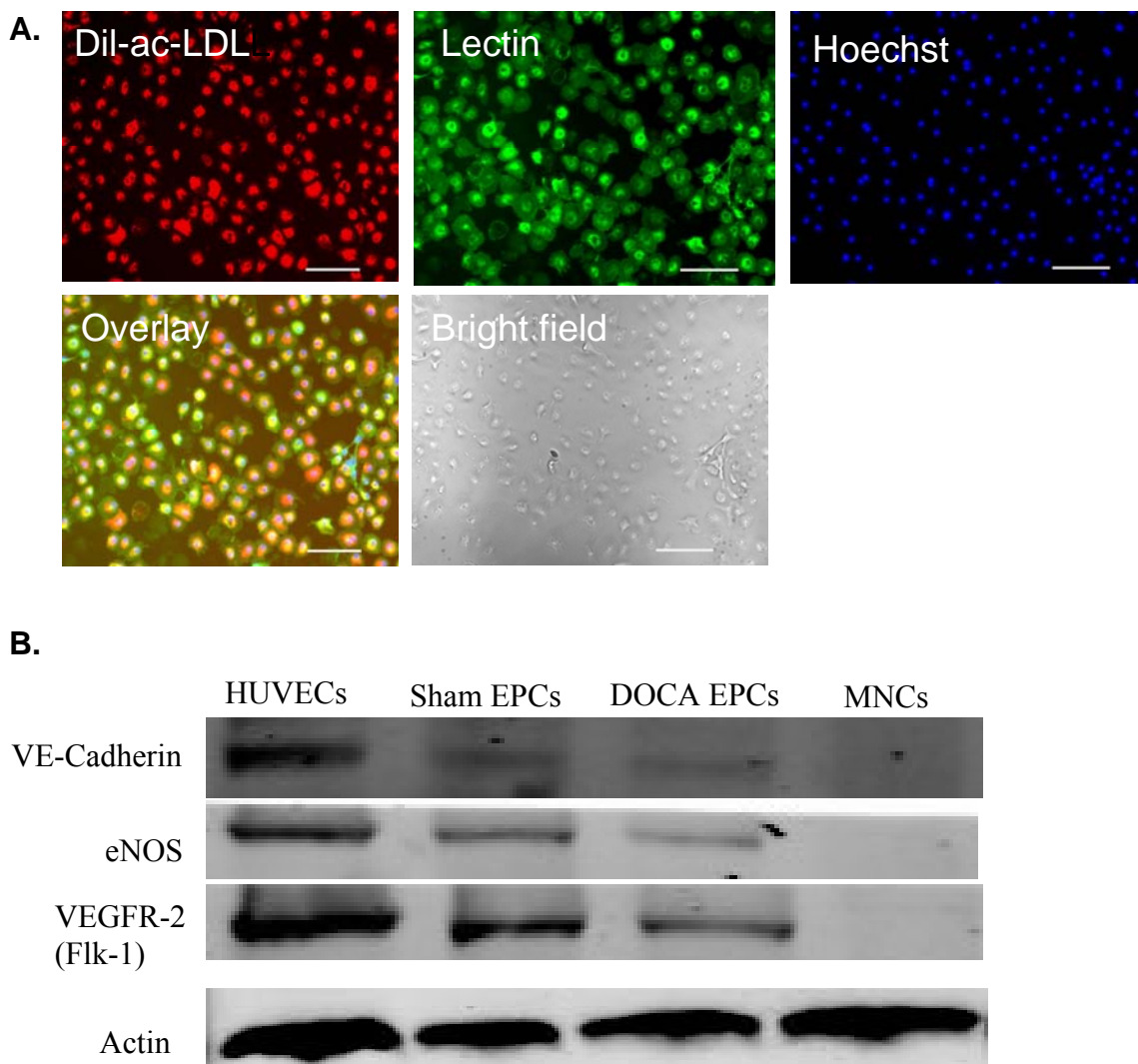


Fig. S1. A. Representative images of Dil-ac-LDL up-taking (red) and lectin binding (green) from circulating EPCs (yellow). The nuclei were stained with Hoechst33258 (blue). After 7 days of cultivation, cells were stained for Dil-ac-LDL uptaking and lectin binding. Dil-ac-LDL/lectin dual positive cells (yellow) were identified as EPCs. Bar=100 μ m. **B. The expressions of endothelial cell specific genes (VE-cadherin, eNOS, and VEGFR-2) in 7-day cultured EPCs.** Human umbilical vein endothelial cells (HUVECs) were used as positive controls.

Fig. S2

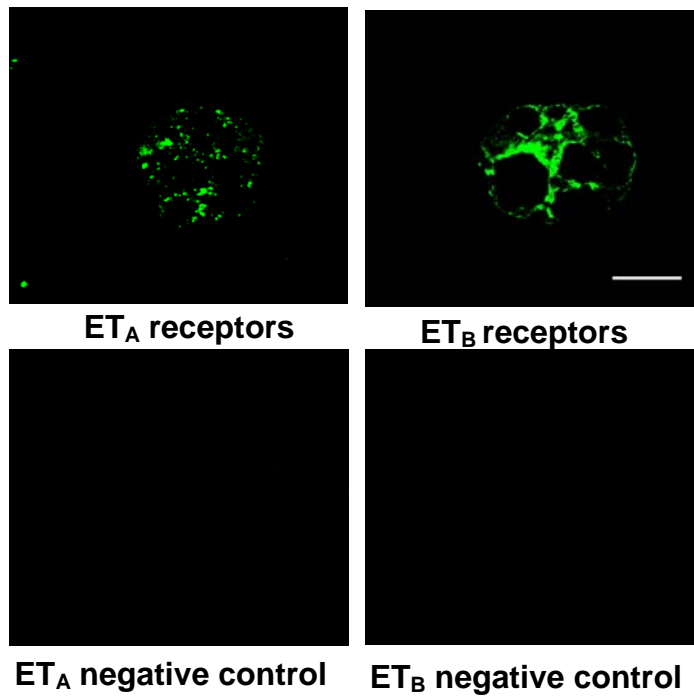
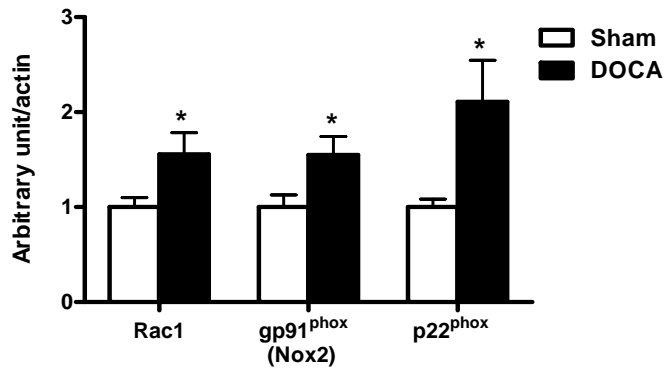
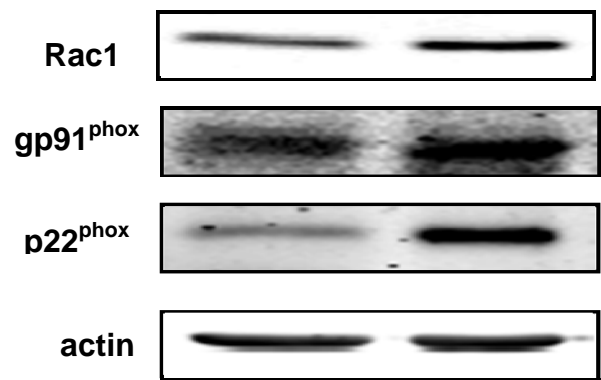


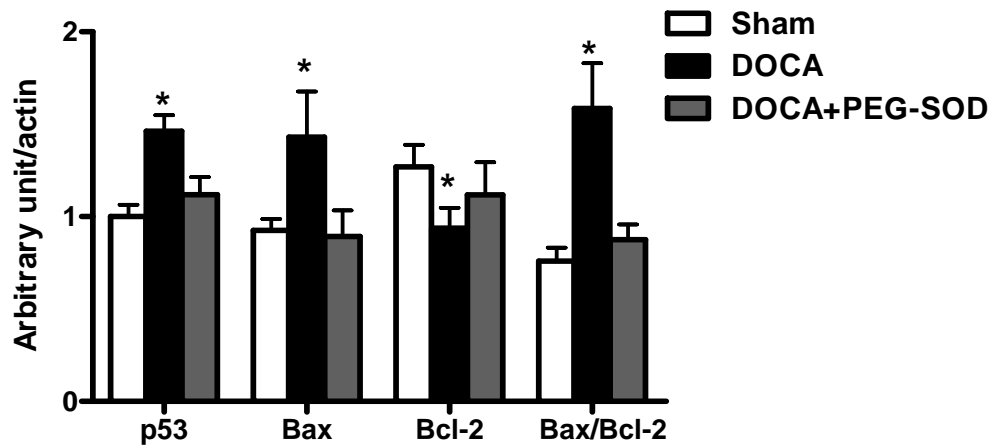
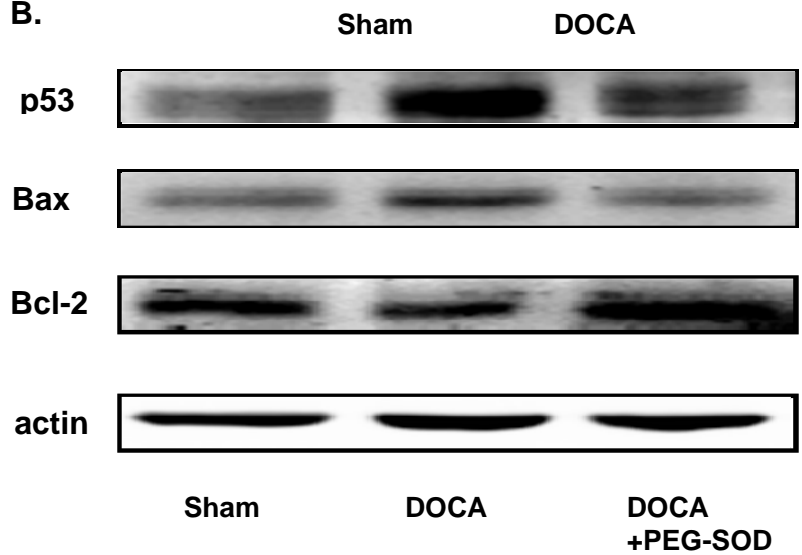
Fig. S2. Representative immunocytochemical images of ET_A and ET_B receptor staining in normal EPCs. The green fluorescence demonstrated expressions of ET_A and ET_B receptors on normal EPCs, respectively. Bar=10 μ m. The second FITC-labeled IgG antibodies were used. To verify the specificity of antibody binding, the primary antibody was incubated with the control peptide prior to application to the cells. The absence of immunoreactivity confirmed the specificity of antibodies for ET receptors.

Fig. S3

A.



B.



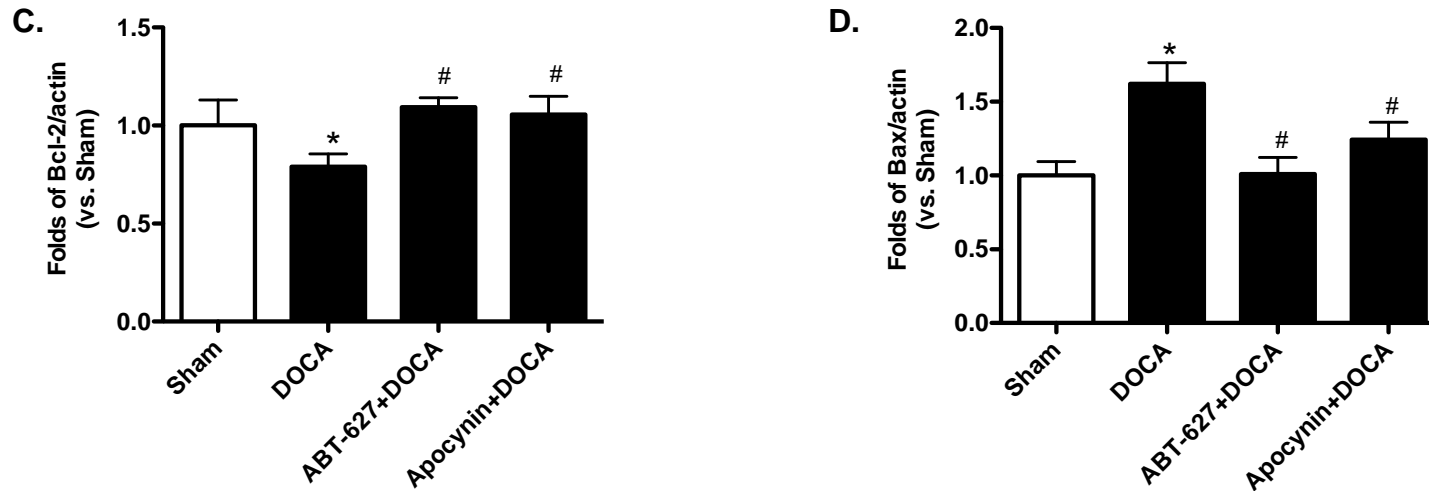


Fig. S3 A. Expressions of NADPH oxidase subunits Rac1, gp91^{phox}, and p22^{phox}. Western blot analysis was performed in cultured EPCs from Sham and DOCA-salt rats. Values were expressed as mean±SEM, which were normalized to Sham rats, n=5-6, **P*<0.05 vs. Sham rats (By a Student's 2-tailed unpaired *t* test). The n values shown representative individual rat. **B. The expressions of p53, Bax, and Bcl-2 EPCs of DOCA-salt rats in the presence or absence of PEG-SOD (100 U/ml, 24 hours).** Values were expressed as mean±SEM, which were normalized to Sham controls, n=4-6, **P*<0.05 vs. Sham rats (By a Student's 2-tailed unpaired *t* test). The n values shown representative individual rat. PEG-SOD: polyethylene glycol-superoxide dismutase, an established membrane-permeable O₂⁻ scavenger. Bax/Bcl-2: the ratio of Bax to Bcl-2. **C and D.** The expressions Bax and Bcl-2 in EPCs of DOCA-salt rats with or without chronic treatments of ET_A receptor blockade (ABT-627, 5 mg·kg⁻¹·d⁻¹) or NADPH oxidase inhibitor (Apocynin, APO, 1.5 mmol/L). The n values shown represented individual rat. Values were expressed as mean±SEM,

Fig. S4

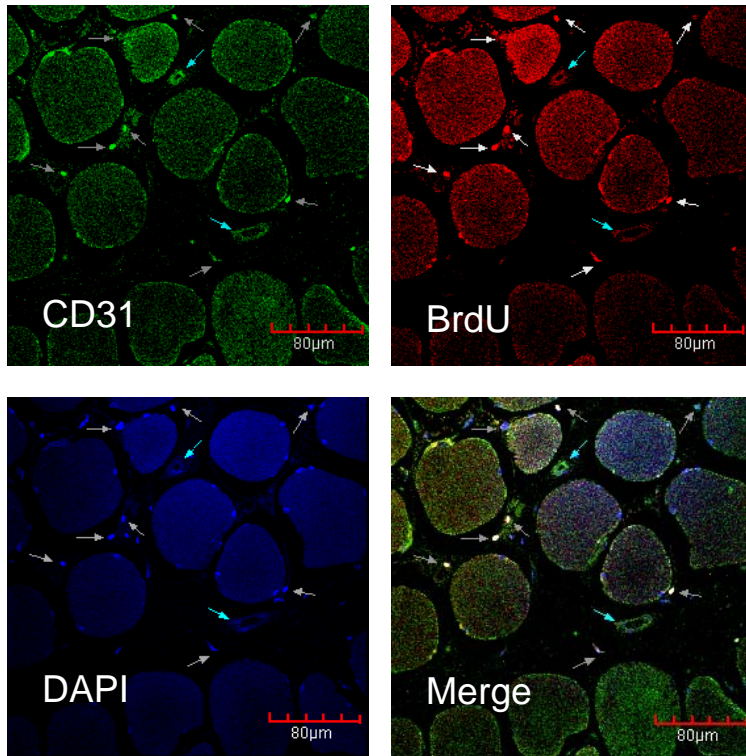


Fig. S4 Representative images of EPC incorporation with vascular culture by confocal microscopy. CD31 indicated endothelial cell (green fluorescence), BrdU indicated implanted EPCs (red fluorescence). The arrows point to the positive staining. DAPI indicated nuclear staining (blue fluorescence).

Fig. S5

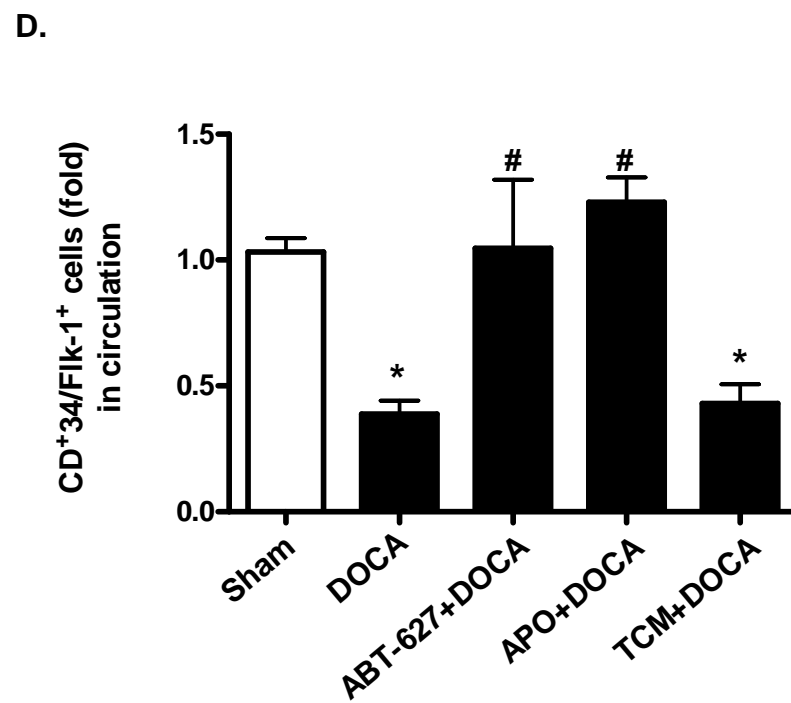
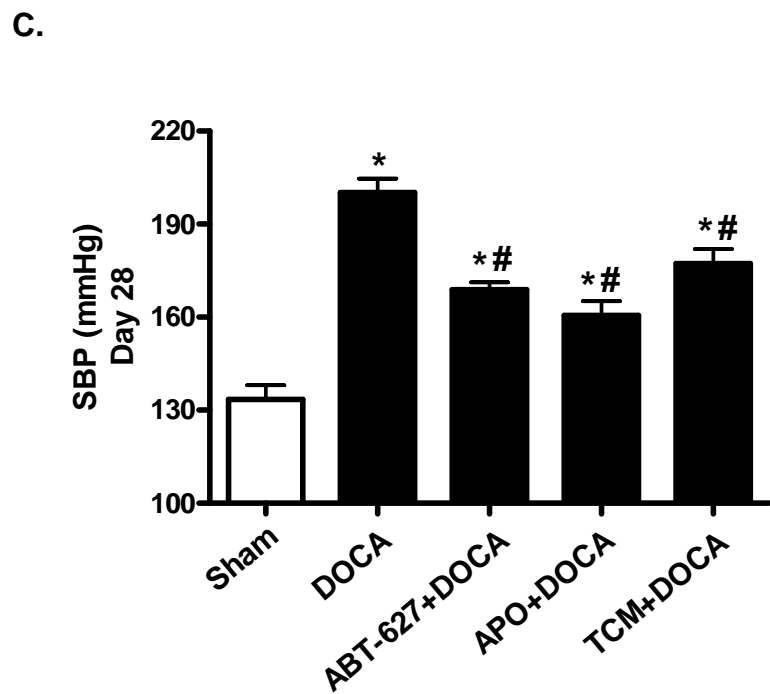
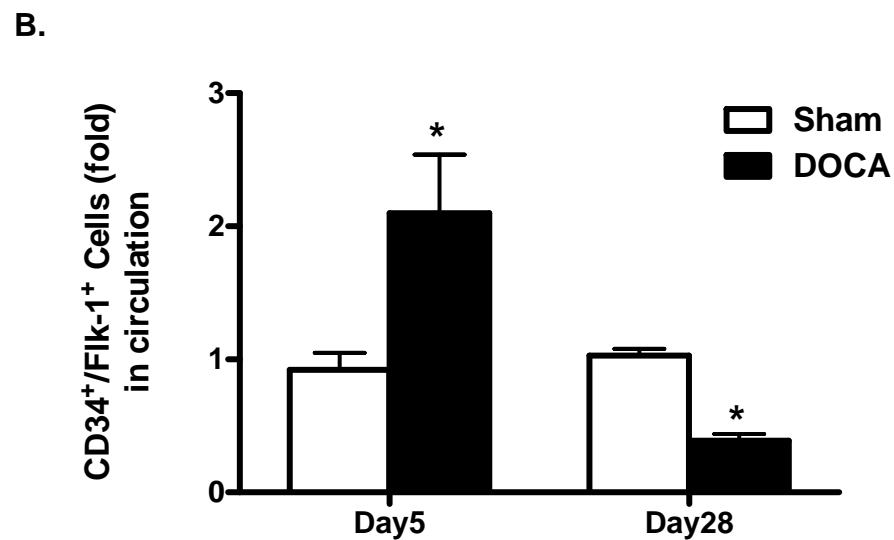
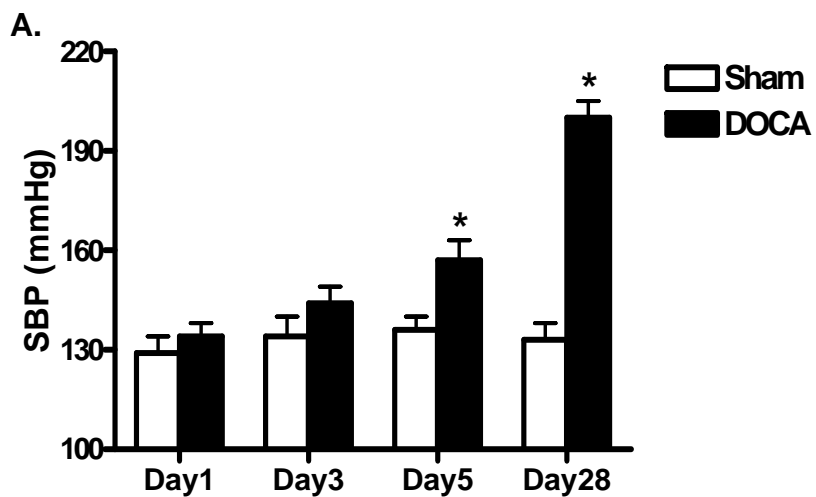


Fig. S5 A. Time course of systolic blood pressure (SBP) in DOCA-salt rats. Values were expressed as mean \pm SEM, n=7-10, * P <0.05 vs. Sham rats (By a Student's 2-tailed unpaired t test). **B. Quantitative analysis of CD34⁺/Flk-1⁺ progenitor cell in circulation on Day 5 and on Day 28 after DOCA-salt regimen.** Freshly isolated peripheral blood mononuclear cells from DOCA-salt and Sham rats were analyzed for the co-expressions of CD34 and Flk-1 by flow cytometry. Values were normalized to Sham rats and expressed as mean \pm SEM, n=6-8, * P <0.05 vs. Sham rats (By a Student's 2-tailed unpaired t test). **C. Effects of ABT-627 (5 mg·kg⁻¹·d⁻¹), apocynin (APO, 1.5 mmol/L) or trichlormethiazide (TCM, 10 mg·kg⁻¹·d⁻¹) on average systolic SBP in DOCA-salt rats.** Values were expressed as mean \pm SEM, n=8-15, * P <0.05 vs. Sham rats, # P <0.05 vs. DOCA rats (By a one-way ANOVA with Bonferroni post-test). ABT-627, a selective ET_A antagonist; APO, an inhibitor of NADPH oxidase; TCM (trichlormethiazide), a diuretic. **D. Effects of ABT-627 (5 mg·kg⁻¹·d⁻¹), Apocynin (APO, 1.5 mmol/L) or trichlormethiazide (TCM, 10 mg·kg⁻¹·d⁻¹) on CD34⁺/Flk-1⁺ progenitor cell levels after DOCA-salt regimen.** Values were normalized to Sham rats and expressed as mean \pm SEM, n=6-8, * P <0.05 vs. Sham rats, # P <0.05 vs. DOCA rats (By a one-way ANOVA with Bonferroni post-test).

Fig. S6

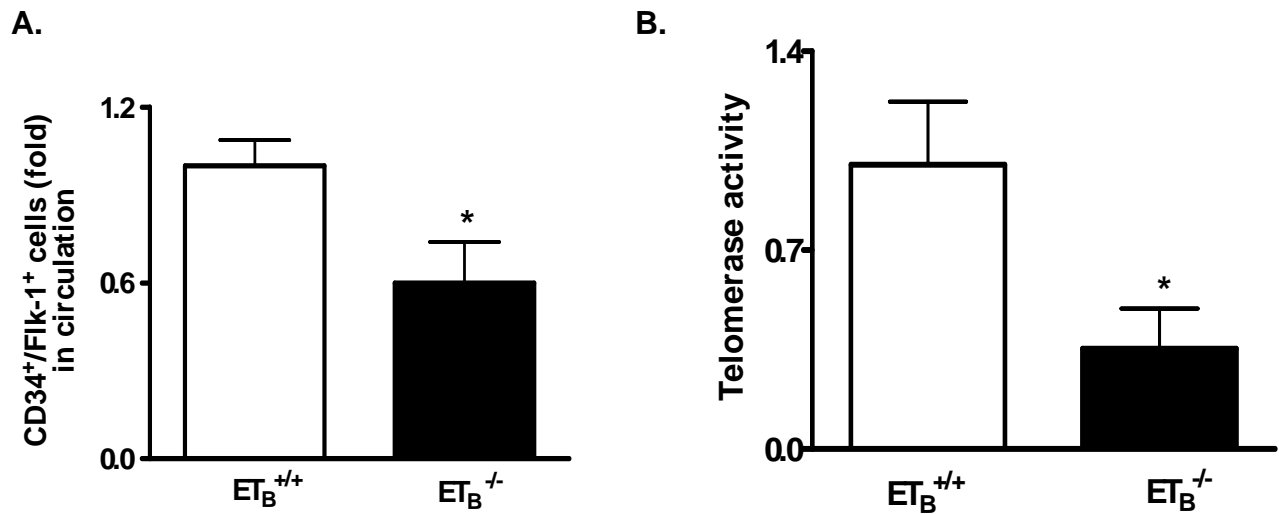


Fig. S6 The circulating progenitor cell number and telomerase activity in ET_B receptor-deficient ($ET_B^{-/-}$) rats. A. The level of $CD34^+/Flk-1^+$ progenitor cells in $ET_B^{-/-}$ rats. Freshly isolated peripheral blood mononuclear cells from $ET_B^{+/+}$ and $ET_B^{-/-}$ rats were analyzed for the co-expressions of CD34 and Flk-1 by flow cytometry. The $CD34^+/Flk-1^+$ progenitor cells were considered as one subpopulation of circulating EPC. Values were normalized to $ET_B^{+/+}$ rats and expressed as mean \pm SEM, n=5-6, * $P < 0.05$ vs. $ET_B^{+/+}$ rats, (By a Student's 2-tailed unpaired t test). **B. EPC telomerase activity was measured by the TRAP assay in $ET_B^{-/-}$ rats.** Seven-day cultured EPCs were used. Values were expressed as mean \pm SEM, n=6. * $P < 0.05$ vs. $ET_B^{+/+}$ rats, (By a Student's 2-tailed unpaired t test).

Fig. S7

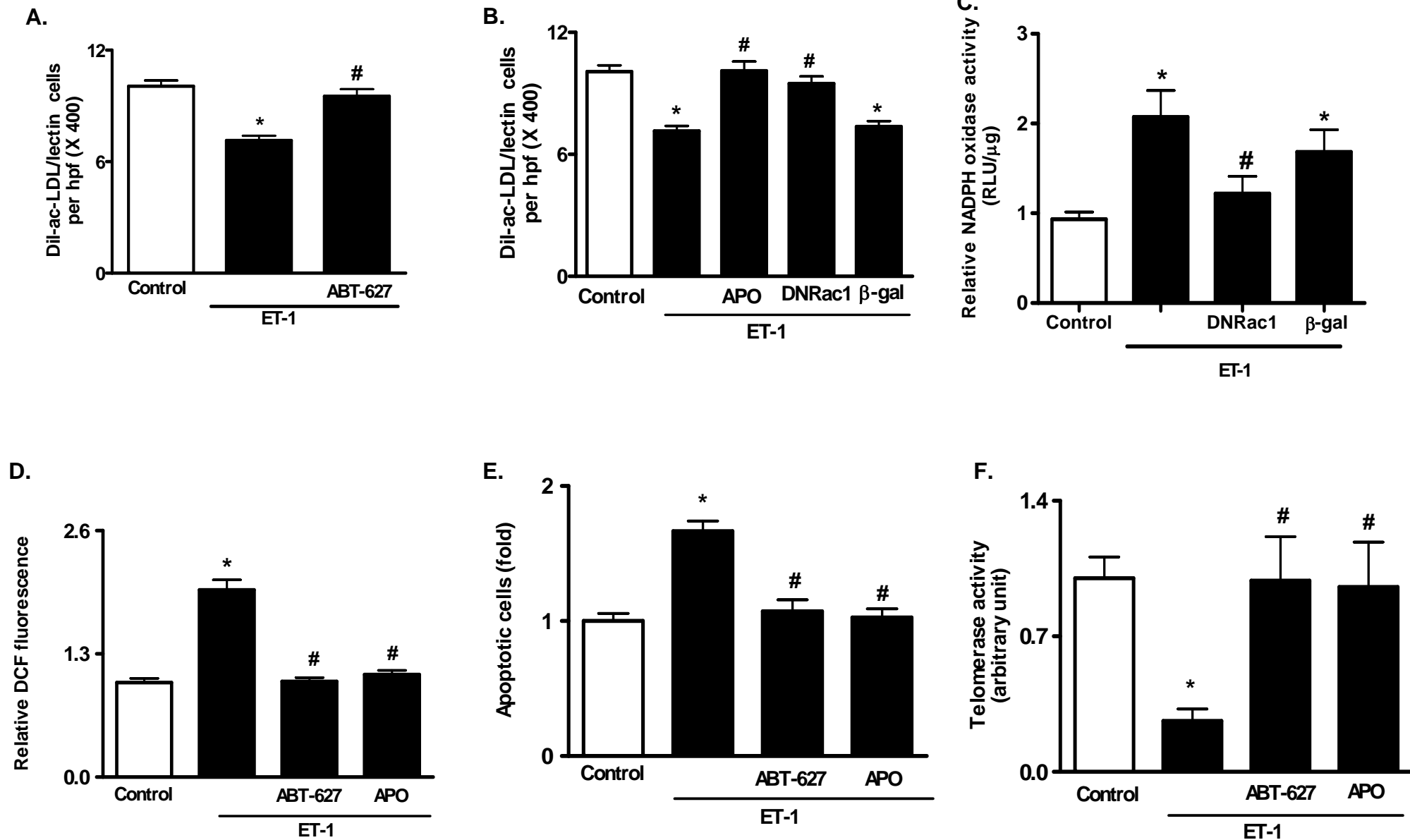


Fig S7. The effects of ET-1 on EPC number, NADPH oxidase activity, ROS level, telomerase activity and apoptosis in normal cultured EPCs. **A. The effect of ET-1 receptor blockade on ET-1 induced EPC reduction.** After cultivation, normal EPCs were pretreated with the selective ET_A receptor antagonist ABT-627 for 1 hour, and then incubated with ET-1 (1×10^{-8} mol/L) for 48 hours. Values were expressed as mean \pm SEM, n=4-6. * $P < 0.05$ vs. Control, # $P < 0.05$ vs. ET-1 treatment only (By a one-way ANOVA with Bonferroni post-test). **B. The effect of NADPH oxidase inhibition on ET-1 induced EPC reduction.** After cultivation, normal EPCs were transfected with AdDNRac1 or Ad β -gal at a titer of 500 multiplicity of infection (MOI) for 24 hours, or pretreated with NADPH oxidase inhibitor Apocynin for 1 hour, followed by a 48-hour treatment with ET-1. Adherent Dil-ac-LDL/lectin dual positive cells were counted as EPCs. Values were expressed as mean \pm SEM, n=4-6. * $P < 0.05$ vs. Control, # $P < 0.05$ vs. ET-1 treatment only or ET-1+ β -gal treatment (By a one-way ANOVA with Bonferroni post-test). **C. The effect of ET-1 on NADPH oxidase activity.** NADPH oxidase activity of EPCs was measured by a lucigenin-enhanced chemiluminescence assay. The enzyme activity was expressed as relative light units (RLU)/ μ g protein. Values were normalized to control group and expressed as mean \pm SEM, n=5-6. * $P < 0.05$ vs. Control, # $P < 0.05$ vs. ET-1 treatment only or ET-1+ β -gal treatment (By a one-way ANOVA with Bonferroni post-test). **D. The effect of ET-1 on EPC intracellular ROS.** ROS level in EPCs was estimated by DCF microscopy. Values were normalized to control groups and expressed as mean \pm SEM, n=4-6, * $P < 0.05$ vs. Control, # $P < 0.05$ vs. ET-1 treatment only (By a one-way ANOVA with Bonferroni post-test). **E. The effect of ET-1 on EPC apoptosis.** Apoptotic EPCs were determined by TUNEL assay. ET-1 (1×10^{-8} mol/L) treated normal EPCs for 48 hours with or without pre-incubation of ET_A receptor antagonist ABT-627 or NADPH oxidase inhibitor Apocynin. Values were normalized to control groups and expressed as mean \pm SEM, n=4-6. * $P < 0.05$ vs. Control, # $P < 0.05$ vs. ET-1 treatment only (By a one-way ANOVA with Bonferroni post-test). **F. The effect of ET-1 on EPC telomerase activity.** Telomerase activity in EPCs was measured by TRAP assay. Values were normalized to control groups and expressed as mean \pm SEM, n=4-6, * $P < 0.05$ vs. Control, # $P < 0.05$ vs. ET-1 treatment only (By a one-way ANOVA with Bonferroni post-test). β -gal: β -galactosidase; DNRac1: dominant-negative Rac1; APO: apocynin.

Fig. S8

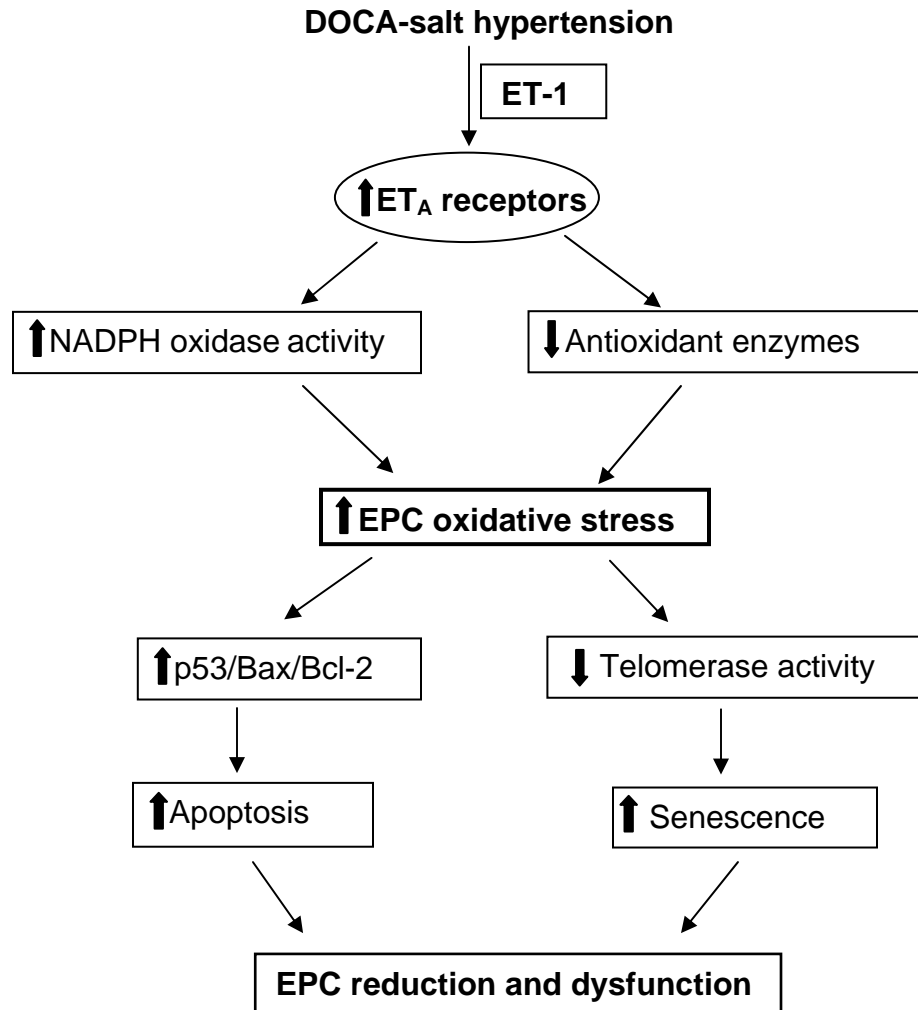


Fig S8. Schematic illustration of possible mechanisms underlying EPC reduction and dysfunction in DOCA-salt hypertension. Endothelin-1 (ET-1) interacts with increased ET_A receptors on endothelial progenitor cells (EPCs), resulting in NADPH oxidase activation and decreased expressions of antioxidant enzymes including MnSOD, CuZnSOD, and GPx-1, which together contribute to ROS accumulation in EPCs of DOCA-salt rats. The elevated ROS may diminish EPC survival by two mechanisms: 1) increased EPC apoptosis via up-regulations of p53 and Bax/Bcl-2 ratio and 2) increased EPC senescence via decreased telomerase activity. Both mechanisms could consequently lead to EPC reduction and dysfunction.